International Journal of Pure and Applied Mathematics
Volume 28 No. 1 2006, 71-84

# 1:4 INTERNAL RESONANCE ACTIVE ABSORBER FOR NON-LINEAR VIBRATING SYSTEM

S. El-Serafi[1], M. Eissa[2], T.H. El-Ghareeb[3] §
[1,2]Department of Engineering Mathematics
Faculty of Electronic Engineering
Menouf, 32952, EGYPT
[3]Department of Mathematics
Faculty of Education
Suez Canal University
Suez, EGYPT
e-mail: taha_elghareeb@yahoo.com

**Abstract:** In this paper we present a mathematical study of active control in some non-linear differential equations, representing a single degree of freedom system like an aircraft wing subjected to multi-excitation forces is considered and solved using the method of multiple scale perturbation. The system is considered with 1:4 internal resonance active control absorber. The approximate solutions are derived up to the second order approximation. The stability of the system is investigated applying both frequency response equations and phase plane methods. The main system vibration can be reduced at the resonance worst case via active control. Some recommendations are given at the end of the work.

**AMS Subject Classification:** 34A34
**Key Words:** control, active, absorber, absorber effectiveness

## 1. Introduction

The main aim of vibrating system analysis, is the study of the vibration nature, the worst resonance cases and to knew the best method for vibration control, i.e.

Received: April 11, 2006

§Correspondence author

reduction or elimination. One of the most effective tools for passive vibration control is the dynamic absorber or the damper or the neutralizer [12]. Eissa [3] has shown that the non-linear absorber widens its range of applications, and its damping coefficient should be kept minimum for better performance [2]. Cheng -Tang Lee et al [10] demonstrated that a dynamic vibration absorber system can be used to reduce speed fluctuations in rotating machinery. Eissa and El-Ganaini [4], [5] studied the control of vibration and dynamic chaos of mechanical structures having quadratic and cubic non-linearities, subjected to harmonic excitation using single and multi-absorbers. Active constrained layer damping (ACLD) has been successfully utilized as effective means of damping out the vibration of various flexible structures [20], [11], [22], [1], [21], [23]. In weakly non-linear systems, internal resonances may occur if the linear natural frequencies are commensurate or nearly commensurate, and internal resonances provide coupling and energy exchange among the vibration modes by Nayfeh et al [13], [18]. If two natural frequencies of a system with quadratic non-linearities are in the ratio 2:1 there exists a saturation phenomenon by Nayfeh et al [13]. When the system is excited at a frequency near the higher natural frequency, the structure responds at the frequency of the excitation and the amplitude of the response increases with the amplitude of the excitation [24]. However, when the high-frequency modal amplitude reaches a critical value, this mode saturates and all additional energy added to the system by increasing the excitation amplitude overflows into the low-frequency mode. Recently the use of internal resonance and saturation phenomena in non-linear control has been extensively studied by Nayfeh et al [9], [14], [16], [15]. This method is based on an approach originally introduced by Golnaraghi [9] and thoroughly investigated in reference [16]. To control transient vibrations, reference [9] used a second-order controller coupled to a vibrating system via quadratic or cubic terms. Nayfeh et al [14], [16] used the saturation phenomenon to successfully control the motion of a d.c. motor with a rigid beam attached.

The authors dealt with 1:3 internal resonance active absorber for non-linear vibrating the same system, the approximate solutions derived, the stability of the system investigated applying both frequency response equations and phase plane methods [6].

The aim of this work is to apply active non-linear vibration absorber using higher-order internal resonances and saturation phenomena to suppress the steady-state vibrations of a cantilever skew aluminum plate [24], [19]. Higher-order internal resonances are introduced using quadratic and cubic terms to couple the controller with the plate. The multiple time scale perturbation technique is applied throughout. An approximate solution is derived. The stability

of the system is investigated applying both frequency response functions (FRFs) and phase-plane methods. The effects of the absorber on system behavior are studied numerically. Optimum working conditions of the system are obtained applying active control methods.

## 2. Mathematical Analysis

The considered equation is the modified non-linear differential equation describing the vibration of an aircraft wing which is given in [17]:

$$\ddot{u}_1 + 2\varepsilon\zeta_1\omega_1\dot{u}_1 + \omega_1^2 u_1 + \varepsilon\beta u_1^3 = \varepsilon g_{12} u_1^2 \dot{u}_1 \dot{u}_2 \ , \tag{1}$$

$$\ddot{u}_2 + 2\varepsilon\zeta_2\omega_2\dot{u}_2 + \omega_2^2 u_2 + \varepsilon\alpha_1 u_2^2 + \varepsilon\alpha_2 u_2^3 = \varepsilon g_1 u_1^2 \dot{u}_1^2 + \varepsilon \sum_{j=1}^{N} F_j \cos(\Omega_j t) \,, \tag{2}$$

where $u_1$ denotes the response of a second-order controller, $\omega_1$ is the natural frequency of the controller, $\zeta_1$ is the damping ratio of the controller, $u_2$ represents one of the modal co-ordinates of a structure, $\omega_2$ is this modal frequency, $\zeta_2$ is the damping ratio, $g_1$ and $g_{12}$ are positive gain constants, $F_j$ are the amplitudes of the external excitation forces, $\Omega_j$ is the external excitation frequency, $\omega_2$ is close to $4\omega_1$, $\Omega_j$ is close to $\omega_2$, $t$ is the time, $\beta$, $\alpha_1$ and $\alpha_2$ are coefficients of stiffness non-linear terms, $\varepsilon$ is a small perturbation parameter. For our considered case we have $N = 2$ for simplicity. The initial conditions are assumed as $u_s(0) = 0.1$ and $\dot{u}_s(0) = 0$, $s = 1, 2$. We seek a first-order approximate solution of equations (1) and (2) using the method of multiple scales [13] in the form

$$u_1(t,\varepsilon) = u_{10} + \varepsilon u_{11} + \varepsilon^2 u_{12} + ... \text{ and } u_2(t,\varepsilon) = u_{20} + \varepsilon u_{21} + \varepsilon^2 u_{22} + ... \,,$$

equating the similar power of $\varepsilon$ leads to

$$(D_0^2 + \omega_1^2)u_{10} = 0 \ , \tag{3}$$

$$(D_0^2 + \omega_2^2)u_{20} = 0 \ , \tag{4}$$

$$(D_0^2 + \omega_1^2)u_{11} = g_{12} u_{10}^2 D_0 u_{10} D_0 u_{20} - 2D_0 D_1 u_{10} - 2\zeta_1\omega_1 D_0 u_{10} - \beta u_{10}^3 \,, \tag{5}$$

$$(D_0^2 + \omega_2^2)u_{21} = g_1 u_{10}^2 (D_0 u_{10})^2 - 2D_0 D_1 u_{20} + \sum_{j=1}^{2} F_j \cos(\Omega_j T_0)$$

$$- 2\zeta_2\omega_2 D_0 u_{20} - \alpha_1 u_{20}^2 - \alpha_2 u_{20}^3 \tag{6}$$

$$\begin{aligned}(D_0^2+\omega_1^2)u_{12} = g_{12}[u_{10}^2(D_0u_{10}D_1u_{20} + D_0u_{10}D_0u_{21} + D_1u_{10}D_0u_{20} \\ + D_0u_{11}D_0u_{20}) + 2u_{10}u_{11}D_0u_{10}D_0u_{20}] - D_1^2u_{10} - 2D_0D_2u_{10} - 2D_0D_1u_{11} \\ - 2\zeta_1\omega_1(D_1u_{10} + D_0u_{11}) - 3\beta u_{10}^2u_{11}\,,\end{aligned} \tag{7}$$

$$\begin{aligned}(D_0^2+\omega_2^2)u_{22} = 2g_1(u_{10}^2(D_0u_{10}D_1u_{10} + D_0u_{10}D_0u_{11}) + u_{10}u_{11}(D_0u_{10})^2) \\ - D_1^2u_{20} - 2D_0D_1u_{21} - 2D_0D_2u_{20} - 2\zeta_2\omega_2(D_1u_{20} + D_0u_{21}) \\ - 2\alpha_1u_{20}u_{21} - 3\alpha_2u_{20}^2u_{21}\,,\end{aligned} \tag{8}$$

where $\frac{d}{dt} = D_0 + \varepsilon D_1 + \varepsilon^2 D_2 + ...$, $D_i = \frac{\partial}{\partial T_i}$, $i = 0, 1, 2, ....$

The general solution of equations (3) and (4) can be expressed in the following forms

$$u_{10}(T_0, T_1, T_2) = A_0(T_1, T_2)e^{i\omega_1 T_0} + cc \quad , \tag{9}$$

$$u_{20}(T_0, T_1, T_2) = B_0(T_1, T_2)e^{i\omega_2 T_0} + cc \ , \tag{10}$$

where $T_n = \varepsilon^n t$ , $n = \{0, 1, 2\}$ are the fast and slow time scales respectively, $A_0$, $B_0$ are a complex function in $T_1$ and $T_2$ and $cc$ represents the complex conjugate. Substituting equation (9) and (10) into equations (5) and (6), yields

$$\begin{aligned}(D_0^2+\omega_1^2)u_{11} = -[3\beta A_0^2\bar{A}_0 + 2i\omega_1(D_1A_0 + \zeta_1\omega_1A_0)]e^{i\omega_1T_0} - \beta A_0^3e^{3i\omega_1T_0} \\ - g_{12}\omega_1\omega_2\bar{A}_0A_0B_0[A_0e^{i(\omega_2+\omega_1)T_0} - \bar{A}_0e^{i(\omega_2-\omega_1)T_0}] \\ - g_{12}\omega_1\omega_2B_0[A_0^3e^{i(\omega_2+3\omega_1)T_0} - \bar{A}_0^3e^{i(\omega_2-3\omega_1)T_0}] + cc\,,\end{aligned} \tag{11}$$

and

$$\begin{aligned}(D_0^2+\omega_2)u_{21} = -[3\alpha_2B_0^2\bar{B}_0 + 2i\omega_2(D_1B_0 + \zeta_2\omega_2B_0)]e^{i\omega_2T_0} - \alpha_2B_0^3e^{3i\omega_2T_0} \\ - [g_1\omega_1^2A_0^4]e^{4i\omega_1T_0} - \alpha_1(B_0^2e^{2i\omega_2T_0} + 2B_0\bar{B}_0) + 2g_1\omega_1^2\bar{A}_0^2A_0^2 \\ + \frac{1}{2}(F_1e^{i\Omega_1T_0} + F_2e^{i\Omega_2T_0}) + cc\,.\end{aligned} \tag{12}$$

From the above-derived solutions, the reported resonance cases are deduced as shown in Table 1.

| Table-1 | | |
|---|---|---|
| No. | Type of Resonances | Case |
| 1 | trivial resonance | $\Omega_1 \cong \Omega_2 \cong \omega_1 \cong \omega_2 = 0$ |
| 2 | primary resonance | $\omega_2 = \omega_1$, $\Omega_1 \cong \omega_2$, $\Omega_2 \cong \omega_2$ |
| 3 | sub-harmonic resonances | $\Omega_1 \cong n\omega_1$, $\Omega_2 \cong n\omega_1$, $\omega_2 = m\omega_1$, $\Omega_1 \cong 2\omega_2$, $\Omega_2 \cong 2\omega_2$, $n = 2, 4$ and $m = 2, 3, 4, 6$ |
| 4 | super-harmonic resonances | $\omega_2 = 2\omega_1/3$, $\omega_1 = 3\omega_2/4$ |

Table 1:

### 2.1. Stability of the System

After studying numerically the different resonance cases, one of the worst cases confirmed numerically has been chosen to study the system stability. The selected resonance case is the primary resonance case where $\Omega_1 \cong \omega_2$ and internal resonance $\omega_2 = 4\omega_1$. In this case we introduce a detuning parameter $\sigma_1$ and $\sigma_2$ such that

$$\omega_2 - 3\omega_1 = \omega_1 + \varepsilon\sigma_1\,, \quad \Omega_1 = \omega_2 + \varepsilon\sigma_2\,. \tag{13}$$

Eliminating the secular term of equations (11) and (12), leads to the solvability conditions for the first order approximation. Using equation (13) and noting that $A_0$ and $B_0$ are a functions in $T_1$ only, we get

$$-[3\beta A_0^2\bar{A}_0 + 2i\omega_1(D_1A_0 + \zeta_1\omega_1A_0)] + g_{12}\omega_1\omega_2\bar{A}_0^3B_0e^{i\sigma_1T_1} = 0\,, \tag{14}$$

$$-[3\alpha_2B_0^2\bar{B}_0 + 2i\omega_2(D_1B_0 + \zeta_2\omega_2B_0)] - g_1\omega_1^2A_0^4e^{-i\sigma_1T_1} + \frac{1}{2}F_1e^{i\sigma_2T_1} = 0\,. \tag{15}$$

Substituting the polar form $A_0 = \frac{1}{2}a_1(T_1)e^{i\gamma_1(T_1)}$ and $B_0 = \frac{1}{2}a_2(T_1)e^{i\gamma_2(T_1)}$ into equations (14) and (15), where $a_1$ and $a_2$ are steady state amplitudes of both the controller and the main system respectively, we get

$$\frac{3}{8}\beta a_1^3 + i\omega_1(a_1' + ia_1\gamma_1' + \zeta_1\omega_1a_1) - \frac{1}{16}g_{12}\omega_1\omega_2a_1^3a_2(\cos\mu_1 + i\sin\mu_1) = 0\,, \tag{16}$$

$$\frac{3}{8}\alpha_2a_2^3 + i\omega_2(a_2' + ia_2\gamma_2' + \zeta_2\omega_2a_2) + \frac{1}{16}g_1\omega_1^2a_1^4(\cos\mu_1 - i\sin\mu_1) - \frac{1}{2}F_1(\cos\mu_2 + i\sin\mu_2) = 0\ , \tag{17}$$

where $\mu_1 = \sigma_1T_1 - 4\gamma_1 + \gamma_2$, $\mu_2 = \sigma_2T_1 - \gamma_2$. For steady state solution $a_1' = a_2' = \mu_1' = \mu_2' = 0$ and separating real and imaginary parts in equations (16) and (17), we get

$$\frac{3}{8}\beta a_1^3 - \frac{1}{4}\omega_1a_1(\sigma_1 + \sigma_2) - \frac{1}{16}g_{12}\omega_1\omega_2a_1^3a_2\cos\mu_1 = 0\,, \tag{18}$$

$$\omega_1^2\zeta_1 a_1 - \frac{1}{16}g_{12}\omega_1\omega_2 a_1^3 a_2 \sin\mu_1 = 0\,, \tag{19}$$

$$\frac{3}{8}\alpha_2 a_2^3 - \omega_2 a_2\sigma_2 + \frac{1}{16}g_1\omega_1^2 a_1^4\cos\mu_1 - \frac{1}{2}F_1\cos\mu_2 = 0\,, \tag{20}$$

$$\omega_2^2\zeta_2 a_2 - \frac{1}{16}g_1\omega_1^2 a_1^4\sin\mu_1 - \frac{1}{2}F_1\sin\mu_2 = 0\,. \tag{21}$$

There are three possibilities in addition to the trivial solution. They are

$$(i)\ a_1 = 0,\ a_2 \neq 0\,.\quad (ii)\ a_1 \neq 0,\ a_2 = 0\,.\quad (iii)\ a_1 \neq 0,\ a_2 \neq 0\,.$$

*Case (i).* $a_1 = 0$, $a_2 \neq 0$. The frequency response equation for this case is

$$\sigma_2^2 - \frac{3\alpha_2 a_2^2}{4\omega_2}\sigma_2 + (\zeta_2^2\omega_2^2 + \frac{9\alpha_2^2 a_2^4}{64\omega_2^2} - \frac{F_1^2}{4\omega_2^2 a_2^2}) = 0\,. \tag{22}$$

Equation (22) is solved numerically and the results are presented by Figures 1(a-d) as the amplitude "$a_2$" against the detuning parameter "$\sigma_2$" for the given values of other parameters. Figures 1(a-d) show the effects of the damping coefficient $\zeta_2$,the non-linear parameter $\alpha_2$, the natural frequency $\omega_2$ and the excitation amplitudes $F_1$ on the steady state amplitude "$a_2$". Figure (1a) shows that the effects of either increasing or decreasing $\zeta_2$ is insignificant. Figure (1b) shows that the positive and negative values of $\alpha_2$, produce either hard or soft spring respectively as the curve is either bent to the right or the left, leading to the appearance of the jump phenomenon which affects fatigue life of the main system. Figure (1c) indicates that the steady state amplitude is monotonic increasing function in $\omega_2$. Figure (1d) shows that the steady state amplitude is a monotonic increasing function in the excitation amplitude $F_1$.

*Case (ii).* $a_1 \neq 0$, $a_2 = 0$. The frequency response equation for this case is

$$\omega_1^2 = \pm\frac{8F_1}{g_1 a_1^4},\quad \sigma_1 + \sigma_2 = \frac{3\beta a_1^2}{2\omega_1}\,. \tag{23}$$

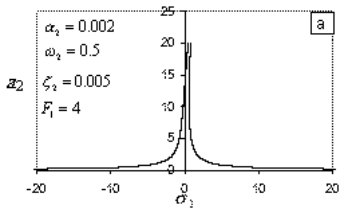


Figure 1a: Effects of the damping coefficient $\xi_2$

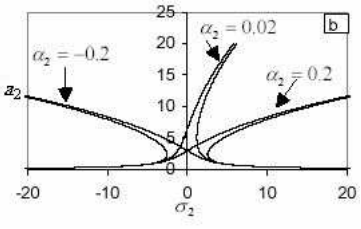


Figure 1b: Effects of non-linear parameter $\alpha_2$

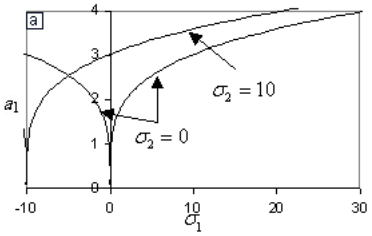


Figure 2a: Effects of the detuning parameter $\sigma_2$

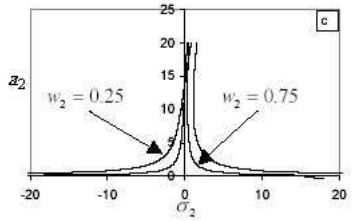


Figure 1c: Effects of the natural frequency $\omega_2$

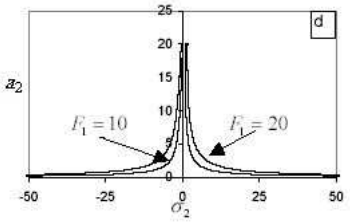


Figure 1d: Effects of the excitation amplitude $F_1$

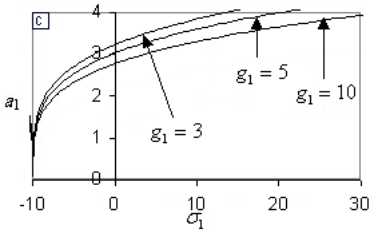


Figure 2c: Effects of the gain $g_1$

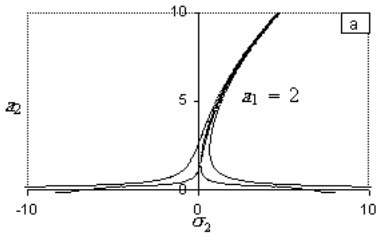


Figure 3a: Effects of the amplitude $a_1 = 2$

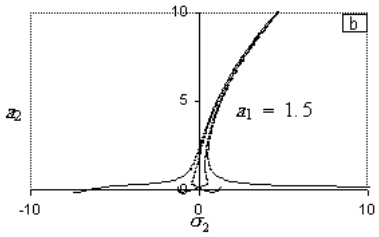


Figure 3b: Effects of the amplitude $a_1 = 1.5$

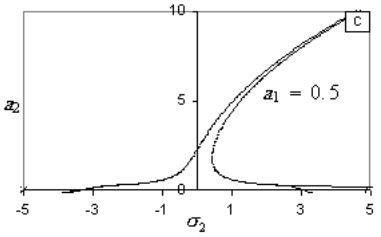


Figure 3c: Effects of the amplitude $a_1 = 0.5$

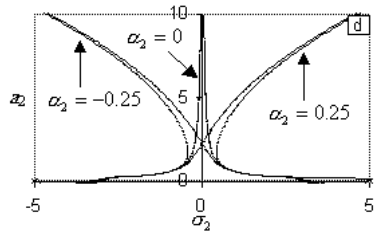


Figure 3d: Effects of non-linear parameter $\alpha_2$

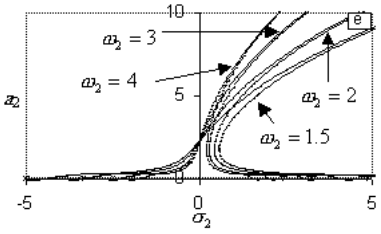


Figure 3e: Effects of the natural frequency $\omega_2$

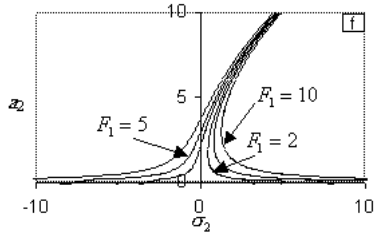


Figure 3f: Effects of the excitation amplitude $F_1$

Equation (23) is solved numerically and the results are presented by Figures 2(a-d) as the amplitude "$a_1$" against the detuning parameter "$\sigma_1$" for the given values of other parameters. Figure 2a shows the effects of the detuning parameter $\sigma_2$, when $\sigma_2$ increasing the curve shifted to the left and bent to the right, leading to the appearance of the jump phenomenon. Figure 2b and Figure 2d show the effects of the non-linear parameter $\beta$, the gain $g_1$ and the excitation amplitudes $F_1$ on the steady state amplitude "$a_1$", where $\sigma_2 = 10$. Figure 2b shows that the non-linear parameter $\beta$, when increasing of $\beta$ the curve is bent to the right. Figure 2c shows that the gain $g_1$, when increasing of $g_1$ the curve is bent to the right. Figure 2d shows that the steady state amplitude is a monotonic decreasing function in the excitation amplitude $F_1$.

*Case (iii).* $a_1 \neq 0$, $a_2 \neq 0$. The frequency response equation for this case

represent by the following equations

$$(\sigma_1 + \sigma_2)^2 - \frac{3\beta a_1^2}{\omega_1}(\sigma_1 + \sigma_2) + (16\zeta_1^2\omega_1^2 + \frac{9\beta^2 a_1^4}{4\omega_1^2} - \frac{g_{12}^2\omega_2^2 a_1^4 a_2^2}{16}) = 0 \ , \quad (24)$$

$$\sigma_2^2 - (\frac{3\alpha_2 a_2^2}{4\omega_2} + \frac{3g_1\beta\omega_1 a_1^4}{4\omega_2^2 a_2^2 g_{12}} - \frac{\omega_1^2 a_1^2 g_1(\sigma_1+\sigma_2)}{2\omega_2^2 a_2^2 g_{12}})\sigma_2 + (\zeta_2\omega_2 - \frac{g_1\zeta_1\omega_1^3 a_1^2}{\omega_2^2 a_2^2 g_{12}})^2 + (\frac{3\alpha_2 a_2^2}{8\omega_2} + \frac{3g_1\beta\omega_1 a_1^4}{8\omega_2^2 a_2^2 g_{12}} - \frac{\omega_1^2 a_1^2 g_1(\sigma_1+\sigma_2)}{4\omega_2^2 a_2^2 g_{12}})^2 - \frac{F_1^2}{4\omega_2^2 a_2^2} = 0 \quad (25)$$

Equations (24) and (25) are solved numerically and the results are presented by Figure 3a – Figure 3f and Figure 4a – Figure 4f as the amplitude "$a_2$" against the detuning parameter "$\sigma_2$" and "$a_1$" against the detuning parameter "$\sigma_1$" for the given values of other parameters. Figure 3a – Figure 3f show the effects of the amplitude $a_1$ in three figures, the non-linear parameter $\alpha_2$, the natural frequency $\omega_2$ and the excitation amplitudes $F_1$ on the steady state amplitude "$a_2$". Figure 3(a-c) show the effects of the amplitude $a_1$ on the steady state amplitude "$a_2$", where $a_1 = 2$, $a_1 = 1.5$, $a_1 = 0.5$. Figure 3d – Figure 3f show the effects of the non-linear parameter $\alpha_2$, the natural frequency $\omega_2$ and the excitation amplitudes $F_1$ on the steady state amplitude "$a_2$", where $a_1 = 0.5$. Figure 3d shows that the negative and positive values of $\alpha_2$, produce either soft or hard spring respectively as the curve is either bent to the right or the left, leading to the appearance of the jump phenomenon. Figure 3e indicates that the steady state amplitude is monotonic decreasing function in the natural frequency $\omega_2$, the curve is bent to the right leading to the occurrence of the jump phenomena. Figure 3f shows that the steady state amplitude is a monotonic increasing function in the excitation amplitude $F_1$. Figure 4a shows that the effects of the steady state amplitude $a_2$, when $a_2$ decreasing the two branches away from each other and the curves are bent to the right; leading to the occurrence of the jump phenomena. Figure 4b shows that the positive and negative values of $\beta$, produce either hard or soft spring respectively as the curves are either bent to the right or the left. Figure 4c shows that the effects of the non-linear parameter $\alpha_2$, when $\alpha_2$ increasing the curves are shifted and bent to the right; leading to the occurrence of the jump phenomena which affects fatigue life of the main system. Figure 4d shows that the effects of the excitation amplitude $F_1$, when $F_1$ increasing the two branches away from each other and the curves are bent to the right; leading to the occurrence of the jump phenomena. Figure 4e shows that the effects of the natural frequency $\omega_1$, when $\omega_1$ decreasing the curves are bent to the right; leading to the occurrence of the

jump phenomena. Figure 4f shows that the effects of the natural frequency $\omega_2$, when $\omega_2$ decreasing the two branches away from each other and the curves are bent to the right; leading to the occurrence of the jump phenomena.

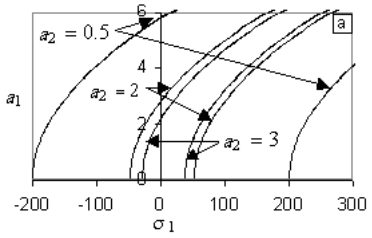


Figure 4a: Effects of the amplitude $a_2$

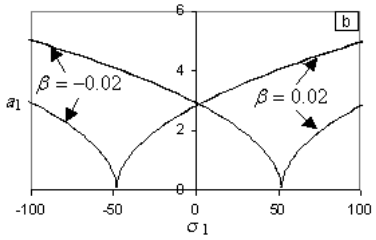


Figure 4b: Effects of non-linear parameter $\beta$

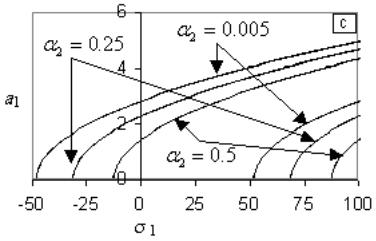


Figure 4c: Effects of non-linear parameter $\alpha_2$

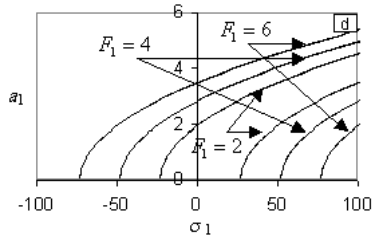


Figure 4d: Effects of the excitation amplitude $F_1$

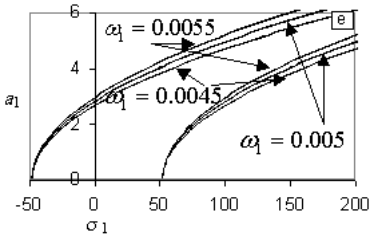


Figure 4e: Effects of the natural frequency $\omega_1$

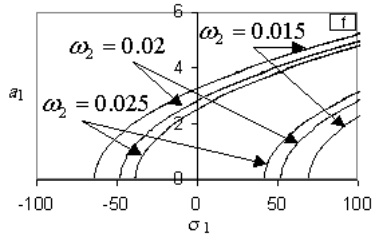


Figure 4f: Effects of the natural frequency $\omega_2$

Figure 5 shows that the system steady state response without absorber at primary resonance is about 50% of the maximum excitation amplitude $F_1$, the system is stable and free of dynamic chaos.

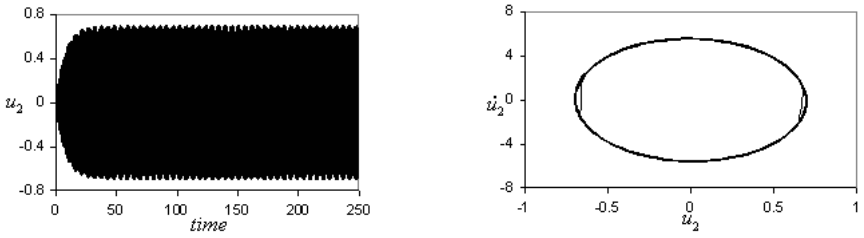


Figure 5: System behavio

### 2.2. Effects of the Absorber

Figure 6 illustrates the response for the system with absorber at the primary resonance $\Omega_1 \cong \omega_2$ and internal resonance $\omega_2 = 4\omega_1$. The effectiveness of the absorber $E_a$ ($E_a$ =amplitude without absorber / amplitude with absorber) is increased to about 5.

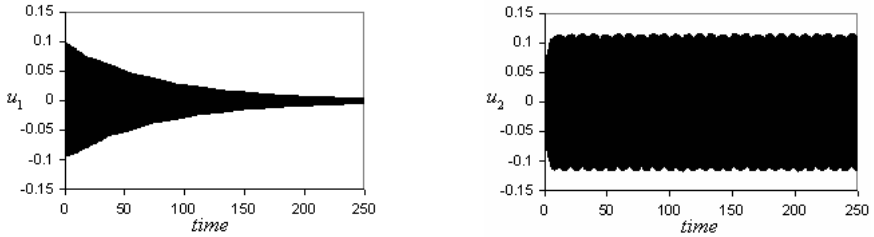


Figure 6: System behavior at

and active absorber $\omega_2 = 4\omega_1$

### 3. Conclusions

The main system of non-linear differential equation representing a single degree of freedom system subjected to multi-excitation force is considered with active absorber 1:4 and solved using the method of multiple scale perturbation. The solution is derived up to second order approximation and the stability of the vibrating system is obtained and studied applying both frequency response function and phase plane method. From the above study the following conclusion may be deduced:

1. The steady state amplitude is a monotonic increasing function to the maximum excitation amplitude $F_1$.

2. The negative and positive values of $\alpha_2$, produce either hard or soft spring respectively as the curve is either bent to the right or the left, leading to the appearance of the jump phenomenon.

3. The steady state amplitude is monotonic decreasing function in the natural frequency $\omega_2$.

4. The steady state response without absorber at primary resonance is about 50% of the maximum excitation amplitude $F_1$, the system is stable and free of dynamic chaos.

5. The effectiveness $E_a$ of the absorber is about 5 at primary resonance where $\Omega_1 = \omega_2$ and $\omega_2 = 4\omega_1$.

It is worth to mention that application of passive control has been dealt with before in reference [6], [7], [8] for similar systems.

## References

[1] A. Baz, M.C. Ray, J. Oh, Active constrained layer damping of thin cylindrical shell, *Journal of Sound and Vibration*, **240**, No. 5 (2001), 921-935.

[2] M. Eissa, Vibration control of non-linear mechanical system via a neutralizer, *Electronic Bulletin*, Faculty of Electronic Engineering Menouf, Egypt, No. 16 (July 1999).

[3] M. Eissa, Vibration and chaos control in I.C engines subject to harmonic torque via non-linear absorbers, In: *ISMV-2000, Second International Symposium on Mechanical Vibrations*, Islamabad, Pakistan (2000).

[4] M. Eissa, El-Ganaini, Part I: Multi absorbers for vibration control of non-linear structures to harmonic excitations, In: *ISMV Conference*, Islamabad, Pakistan (2000).

[5] M. Eissa, El-Ganaini, Part II: Multi absorbers for vibration control of non-linear structures to harmonic excitations, In: *ISMV Conference*, Islamabad, Pakistan (2000).

[6] S. El-Serafi, M. Eissa, H. El-Sherbiny, T.H. El-Ghareeb, 1:3 internal resonance active absorber for non-linear vibrating System, *Institute of Mathematics and Computer Sciences*, To Appear.

[7] S. El-Serafi, M. Eissa, H. El-Sherbiny, T.H. El-Ghareeb, Comparison between passive and active control of non-linear dynamical system, *Japan Journal of Industrial and Applied Mathematics*, To Appear.

[8] S. El-Serafi, M. Eissa, H. El-Sherbiny, T.H. El-Ghareeb, On passive and active control of vibrating system, *International Journal of Applied Mathematics*, To Appear.

[9] M.F. Golnaraghi, Regulation of flexible structures via non-linear coupling, *Journal of Dynamics and Control*, **1** (1991), 405-428.

[10] Cheng-Tang Lee et al., Sub-harmonic vibration absorber for rotating machinery, *ASME Journal of Vibration and Acoustics*, **119** (1997), 590-595.

[11] N. Liu, K.W. Wang, A non-dimensional parametric study of enhanced active constrained layer damping treatments, *Journal of Sound and Vibration*, **223**, No. 4 (1999), 611-644.

[12] J.D. Mead, *Passive Vibration Control*, John Wiley and Sons (1999).

[13] A.H. Nayfeh, D.T. Mook, *Non-Linear Oscillations*, New York, Wiley (1979).

[14] S.S. Oueini, A.H. Nayfeh, *Saturation Control of a DC Motor*, AIAA-96-1642-CP (1996).

[15] S.S. Oueini, M.F. Golnaraghi, Experimental implementation of the internal resonance control strategy, *Journal of Sound and Vibration* (1997).

[16] S.S. Oueini, A.H. Nayfeh, M.F. Golnaraghi, A theoretical and experimental implementation of a control method based on saturation, *Non-Linear Dynamics*, **13** (1997), 189-202.

[17] P.F. Pai, R. Bernd, M.J. Schilz, Non-linear vibration absorbers using higher order internal resonances, *Journal of Sound and Vibration*, **234**, No. 5 (2000), 799-817.

[18] P.F. Pai, A.H. Nayfeh, Three-dimensional non-linear vibrations of composite beams-II, *Flapwise Excitations, Non-Linear Dynamics*, **2** (1991), 1-34.

[19] P.F. Pai, M.J. Schilz, A refined non-linear vibration absorber, *International Journal of Mechanical Sciences*, **42** (2000), 537-560.

[20] I.Y. Shen, Weili Guo, Y.C. Pao, Torsional vibration control of a shaft through active constrained layer damping treatments, *Journal of Vibration and Acoustics*, **119** (1997), 504-511.

[21] Y.M. Shi, Z.F. Li, X.H. Hua, Z.F. Fu, T.X. Liu, The modeling and vibration control of beams with active constrained layer, *Journal of Sound and Vibration*, **245**, No. 5 (2001), 785-800.

[22] R. Stanawy, D. Chantalkhana, Active constrained layer damping of clamped-clamped plate vibration, *Journal of Sound and Vibration*, **241**, No. 5 (2001), 755-777.

[23] D. Sun, L. Tong, Modeling and vibration control of beams with partially de-bonded active constrained layer damping patch, *Journal of Sound and Vibration*, **252**, No. 3 (2002), 493-507.

[24] B. Wen, A.S. Naser, M.J. Schulz, Structural vibration control using PZT patches and non-linear phenomena, *Journal of Sound and Vibration*, **215**, No. 2 (1998), 273-296.